Desalination and Water Treatment
www.deswater.com

doi: 10.5004/dwt.2020.26257

204 (2020) 366–376
November

Cyanopropyl-functionalized nanosilica based dispersive micro-solid phase extraction method for rapid removal of organophosphorus pesticides from water samples

Zahra Sotoudehnia Korrani[a], Abdolhamid Alizadeh[b,*], Wan Aini Wan Ibrahim[a,c,*], Gaurav Sharma[d,*]

[a]*Medical Education Development Center, Sirjan School of Medical Sciences, Sirjan, Iran, email: zahrasetoudehnia@yahoo.com (Z.S. Korrani)*
[b]*Department of Organic Chemistry, Faculty of Chemistry, Razi University, Kermanshah, 6714967346 Iran, email: ahalizadeh2@hotmail.com (A. Alizadeh)*
[c]*Center for Sustainable Nanomaterials, Ibnu Sina Institute for Scientific and Industrial Research, Universiti Teknologi Malaysia, 81310 UTM, Johor Bahru, Johor, Malaysia, email: wanaini@kimia.fs.utm.my (W.A.W. Ibrahim)*
[d]*School of Chemistry, Shoolini University, Solan – 173212, Himachal Pradesh, India, email: gaurav8777@gmail.com (G. Sharma)*

Received 4 December 2019; Accepted 13 June 2020

ABSTRACT

In this study, a hydrophilic adsorbent based on cyanopropyl-functionalized silica nanoparticles (CNPr@SiO_2 NPs) was successfully synthesized via a sol–gel method. The nanoparticles were characterized using Fourier transform infrared spectroscopy, field emission scanning electron microscopy, Brunauer–Emmett–Teller analysis, and thermogravimetric analysis. The synthesized CNPr@SiO_2 NPs were then used as an adsorbent in dispersive micro-solid phase extraction (D-µ-SPE) of some polar and nonpolar organophosphorus pesticides from water samples prior to high-performance liquid chromatography-ultraviolet detection. Under the optimized parameters, the proposed method based on CNPr@SiO_2 NPs showed low limits of detection in the range of 0.047–0.059 µg L^{-1}, satisfactory recoveries (101.21%–109.12%), and good RSDs (0.20%–6.70%) for the extraction of OPPs from the various water samples. In addition, the developed D-µ-SPE method based on CNPr@SiO_2 NPs showed a superior extraction capability toward the OPPs in comparison to commercial cyanopropyl-bonded silica solid-phase extraction cartridge.

Keywords: Silica nanoparticles; Cyano-functionalized nanosilica; Dispersive micro-solid phase extraction; Organophosphorus pesticides

---

1. Introduction

Pesticides are a large group of hazardous organic compounds that are utilized on farms as herbicides, fungicides, and insecticides [1–4]. Organophosphorus pesticides (OPPs) are extensively applied in agriculture to protect crops from insects damage and improve their quantity and quality [5,6]. However, their residues are a major source of environmental contamination, as they can be migrated from soil and air into the water resources during their usage. The United States Environmental Protection Agency (US-EPA) has classified most of OPPs as highly or moderately toxic substances [7,8]. According to the established regulation by the European Union (EU Directive 98/83/EC), the maximum acceptable level for individual and total pesticides in drinking water is 0.10 and 0.50 µg L^{-1}, respectively [9]. Due

---

* Corresponding authors.

1944-3994/1944-3986 © 2020 Desalination Publications. All rights reserved.

to toxicity and biomagnification of OPPs residue, development of accurate, and sensitive methods for monitoring and detecting the trace amount of OPPs in water sources are essential. Various sample preparation techniques such as dispersive liquid–liquid microextraction (DLLME) [10,11], solid phase extraction (SPE) [12–14], solid phase microextraction (SPME) [15,16], stir bar sorptive extraction (SBSE) [17], and magnetic solid phase extraction (MSPE) [6,18] have been developed for extracting of OPPs.

None of the above-mentioned techniques has revealed to be superior to the other and some of them suffer from various drawbacks such as tedious and time-consuming sample preparation steps, and failure to extract polar compounds from water, etc. However, among the mentioned techniques, SPE is currently well-established as a simple and powerful sample pre-concentration and clean-up method, due to its many advantages such as simplicity, good efficiency, high sensitivity, easy automation, low consumption of reagents and solvents, reusability of the adsorbent, and flexible to combine with other instrumental techniques in an online or off-line mode [19]. But, this technique is time-consuming because of its limited mass transfer rate and there is also probability of the cartridge blockage [20]. To overcome the traditional SPE limitations, many new methodologies have been designed. Recently, a new mode of SPE with potential benefits called dispersive micro-solid phase extraction (D-μ-SPE) has been developed [21–23]. This technique compared to common SPE is simpler and faster and requires a limited amount of the adsorbent. In this technique, unlike the conventional SPE, the adsorbent is not packed into the cartridge and directly added to the sample solution containing target analytes.

In the D-μ-SPE technique, the type of the adsorbent is a critical parameter as it determines the adsorption capacity, selectivity, and sensitivity toward the analytes. In the past decade, nanoscale solid materials have gained increasing attention because of their unique properties including high activity and high surface area [24]. The potential ability of NPs as adsorbent materials in separation science has been extensively studied for several years [25,26]. Compared with micro-sized particles used for SPE based methods, nano-sized materials not only have a significantly higher specific surface area that provides much higher extraction capacity and efficiency but also can be easily modified with various functionalities which improve their selectivity. Silica nanoparticles are one of the most frequently used because of their low cost, accessibility, good mechanical and thermal stability, and flexibility in further surface functionalization [27]. Modified silica nanoparticles have been used as an effective adsorbent for sample preparation of various pollutants such as pesticides [28], polycyclic aromatic hydrocarbons [29], bisphenol A [30], and heavy metals [31,32], and satisfactory results have been achieved. Among different established methods for preparation of silica nanoparticles, the sol–gel technique has attracted great interest due to its simplicity, the capability to control the particle size, purity of the products, and the mild synthesis conditions [33,34].

This study focused on the functionalization of silica nanoparticles with polar cyanopropyl moieties (CNPr@SiO_2 NPs) that was tailored for use as a D-μ-SPE adsorbent. The synthesized nanosorbent was then successfully applied to the extraction and preconcentration of three selected polar and nonpolar OPPs from aqueous media. Moreover, the laboratory synthesized nanomaterial revealed superior analytical performance toward the target OPPs compared to commercial cyano-bonded silica SPE cartridge.

2. Experimental

2.1. Reagents and materials

Methanol (high-performance liquid chromatography (HPLC) grade), ethanol, toluene, and *n*-hexane were purchased from Merck (Darmstadt, Germany). Hydrochloric acid (HCl, 37.5%) and dichloromethane (DCM) were purchased from Fluka (Buchs, Switzerland). Cyanopropyltriethoxysilane (CNPrTEOS), tetraethoxysilane (TEOS), and ammonium hydroxide (NH_4OH, 25%), and analytical grade standard of OPPs (dicrotophos, chlorpyrifos, and diazinon) were supplied by Sigma-Aldrich (St. Louis, MO, USA). Purified water was produced by a Simplicity 185 UV system (Millipore, MA, USA). Pesticide stock solutions (1,000 ppm) were prepared by dissolving an appropriate amount of each compound in HPLC grade methanol and stored at –20°C in the refrigerator until to use. The working solutions were prepared freshly by diluting the stock solution with ultrapure water before the experiments. The commercial cyano 100 mg/1 mL SPE cartridge was purchased from Supelco (Bellefonte, PA, USA).

2.2. Instrumentation

2.2.1. Liquid chromatography

HPLC analysis of the OPPs was carried out using an Agilent 1100 series HPLC (Agilent Technologies, USA) consisting of a vacuum solvent degasser, a manual injector with a 10 μL Rheodyne loop (Rheodyne, Cotati, CA, USA) and an ultraviolet detector. The OPPs separation was achieved on an Eclipse XDB-C18 column (150 mm × 4.6 mm I.D., 5 μm particle size, Agilent Technologies, Santa Clara, CA, USA) at 40°C. The mobile phase consisted of a mixture of methanol and water (70:30, v/v) eluted at a flow rate of 1.0 mL min^{-1} with UV detection at 270 nm. The mobile phase was filtered through a Millipore 0.22 μm membrane filter and degassed prior to use.

2.2.2. Characterization

The infrared spectra were recorded using the KBr pellets on a Perkin Elmer 1600 series Fourier transform infrared (FTIR) spectrophotometer (MA, USA) in the range of 400–4,000 cm^{-1}. The surface morphology of the adsorbent was investigated using a field emission JSM-6710F scanning electron microscopy (SEM; JEOL, Tokyo, Japan). The Brunauer–Emmett–Teller (BET) surface area and pore size of the synthesized material were determined by using nitrogen adsorption–desorption analysis with an ASAP 2010 Micromeritics instrument (Delta Analytical Instrument Inc., Bellefonte, PA, USA) at 77 K and by the BET method. Thermal stability studies were performed with a Perkin-Elmer model TGA 7 thermogravimetric analyzer (Perkin-Elmer Corporation, USA) at a heating rate of 10°C min^{-1} under a nitrogen atmosphere.

2.3. Preparation of cyanopropyl functionalized silica nanoparticles

2.3.1. Synthesis of silica nanoparticles

The silica nanoparticles (SiO_2 NPs) were obtained using the sol–gel method. Firstly, 8 mL of TEOS was added to a mixture of water (25 mL) and ethanol (15 mL) in a 250 mL beaker and stirred for 5 min. Then, 1 mL of NH_4OH (pH 12) was added dropwise into the mixture and magnetically stirred for 1 h at room temperature to form a white transparent homogeneous solution. The prepared solution was kept for 4 h until the gel was formed. The particles were separated by filtration, washed with 40 mL of deionized water and dried at 80°C for 1 d.

2.3.2. Synthesis of CNPr@SiO_2 NPs

The SiO_2 NPs were firstly activated through refluxing the particles in concentrated HCl (6 M) for 6 h. Then SiO_2 NPs were filtered and washed with excess distilled water and oven-dried at 90°C for 24 h. Next, 1.0 g of dried activated SiO_2 NPs and 2.5 mL of 3-cyanopropyltriethoxysilane were dissolved in 30 mL of anhydrous toluene. The solution was again refluxed at 100°C for 24 h under nitrogen gas, filtered and subsequently washed with toluene, dichloromethane, and methanol. Finally, the obtained material was dried under vacuum at 80°C for 8 h. Finally, cyanopropyl functionalized silica nanoparticles (CNPr@SiO_2 NPs) were obtained.

2.4. Dispersive micro-solid phase extraction procedure

In this procedure, 50 mg of the CNPr@SiO_2 NPs were added into a beaker containing 150 mL of OPPs aqueous solution (50 μg L^{-1}). The sample was shaken by an orbital shaker at 250 rpm for 10 min. The solution was then centrifuged for 3 min at 5,000 rpm and the supernatant was discarded. The adsorbent was transferred into a 2 mL safe lock tube and the target analytes were desorbed by ultrasonication for 3 min using 150 μL of dichloromethane. The dichloromethane was filtered and dried under a gentle stream of nitrogen gas. Finally, the residue was reconstituted in 60 μL of methanol, and 10 μL of it was injected into the HPLC-UV for analysis.

2.5. Column SPE procedure

The commercial Cyano-SPE cartridge was connected to a 12-port Visiprep SPE vacuum manifold (Supelco, Bellefonte, PA, USA) and conditioned sequentially with 5 mL methanol, and 10 mL deionized water. The 5 mL sample solution (containing 50 μg L^{-1} of each OPPs) was passed through the cyano-cartridge at a flow rate of 0.5 mL min^{-1}. After drying the cartridge, the pesticides were eluted from the adsorbent with 4 mL dichloromethane. The extract was then evaporated to dryness under a gentle stream of nitrogen gas, redissolved in 60 μL methanol, and filtered through a syringe filter PTFE of 0.45 μm prior to HPLC-UV analysis. Finally, 10 μL of the filtrate was injected into the HPLC system. In order to achieve the best extraction conditions, three main parameters affecting extraction including the solvent type, the volume of desorption solvent, and the sample volume were studied. The optimum SPE conditions for commercial Cyano-SPE adsorbent were 5 mL sample loading and 4 mL dichloromethane as the eluting solvent.

2.6. Real samples preparation

Bottled mineral water and bottled drinking water were purchased from a local market. Tap water was obtained from our laboratory, and river water samples were taken from the university lake (UTM). The water samples were filtered using a 0.2 μm pore size nylon membrane before analysis. For recovery analysis, the water samples were spiked with a mixture of OPPs standard at 0.2 μg L^{-1} for prepared CNPr@SiO_2 NPs and at 5 μg L^{-1} for the commercial cyano-bonded silica particles.

3. Results and discussion

3.1. Characterization of the CNPr@SiO_2 NPs

Surface functional groups of the pristine TEOS, as prepared SiO_2 NPs, pristine CNPrTEOS and CNPr@SiO_2 NPs nanocomposite were studied with FTIR as shown in Figs. 1A–D. The FTIR spectra of TEOS (Fig. 1A) show two main peaks for methyl bond (C–H) at 2,930 cm^{-1} and Si–O stretching at 1,100 cm^{-1}. Fig. 1B is for SiO_2 NPs with Si–O (1,100 cm^{-1}) and O–H (3,390 and 1,634 cm^{-1}) groups, which correspond to O–H bond stretching vibration of the absorbed water and the O–H of the Si–O–H groups. Fig. 1C is confirms C≡N stretching bond at 2,246 cm^{-1} for CNPrTEOS. The FTIR spectrum of CNPr@SiO_2 NPs (Fig. 1D) shows peaks at 3,390 and 1,634 cm^{-1} for O–H stretching, Si–O stretching band appears at approximately 1,100 cm^{-1} and the C≡N stretching at 2,246 cm^{-1}. This indicates the successful functionalization of SiO_2-NPs with cyano groups (C≡N) using the CNPrTEOS precursor.

The surface morphology of the CNPr@SiO_2 NPs was investigated using FESEM (Fig. 2). The FESEM image exhibited the well-distributed spherical particles with the average particle size of approximately 30 nm. The elemental composition of the CNPr@SiO_2 NPs was also evaluated by field emission scanning electron microscopy with energy dispersive X-ray spectroscopy (FESEM-EDX). According to the FESEM-EDX analysis of the CNPr@SiO2 NPs as shown in Fig. 2, four elements including carbon (43.2%), nitrogen (16.3%), oxygen (27.7%), and silicon (12.6%) were present in the prepared CNPr@SiO2 NPs.

The physical structure of the CNPr@SiO_2 NPs was analyzed using nitrogen adsorption–desorption isotherm with BET method and the corresponding Barrett–Joyner–Halenda (BJH) pore size distribution. The isotherm of CNPr@SiO_2 NPs was placed in the type IV isotherm class with a distinct hysteresis loop. This type of N_2 adsorption–desorption isotherm is normally acquired from mesoporous materials based on the International Union of Pure and Applied Chemistry classifications [35,36]. The surface area of the synthesized CNPr@SiO_2 was measured as 570 m^2 g^{-1} and the average pore diameter was found to be 3.56 nm (by the BJH method) confirming the mesoporous structure of the adsorbent.

Fig. 3 depicts the TGA curves of the CNPr@SiO_2 sorbent and SiO_2 NPs over the temperature range of 50°C–800°C. The SiO_2 NPs and CNPr@SiO_2 exhibited high thermal

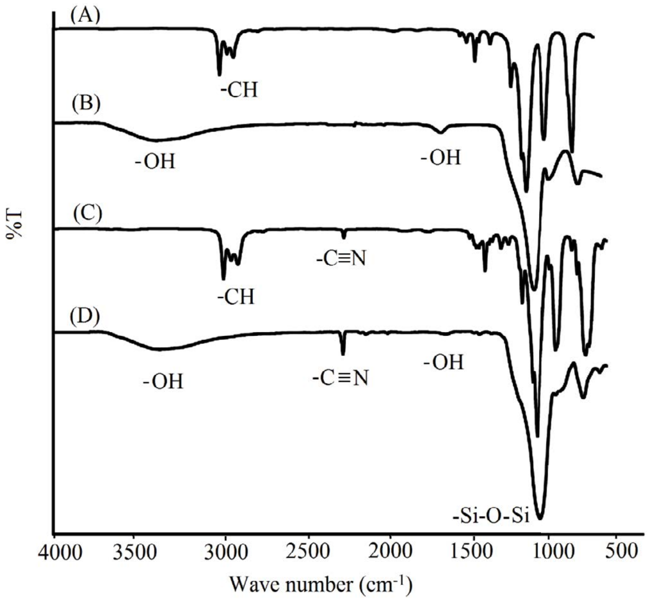

Fig. 1. FTIR spectra of (A) TEOS, (B) synthesized SiO_2 NPs, (C) CNPrTEOS, and (D) synthesized CNPr@SiO_2 NPs.

stabilities from 100°C to 800°C and 100°C to 400°C, respectively. According to the thermal degradation of the SiO_2-NPs (Fig. 3A), single weight loss stage is detected below 100°C. The thermal degradation of the CNPr@SiO_2 (Fig. 3B) showed two weight loss stages one below 100°C and one between 400°C and 600°C. The CNPr@SiO_2 was stable after 600°C. The weight loss below 100°C could be due to the evaporation of a small amount of surface adsorbed water molecules and thermal decomposition of any organic solvent remnants. Between 400°C and 600°C, the weight loss could be attributed to the decomposition and destruction of the organic compounds (carbon, hydrogen, and oxygen) bound onto silica NPs.

3.2. Mechanism of the synthesis process

Preparation of CNPr@SiO_2 NPs consisted of two synthesis process: first is the synthesis of silica nanoparticles, and the second includes the functionalization of silica NPs with CNPrTEOS. The synthesis of the SiO_2-NPs was based on the two steps: hydrolysis and condensation of silicon alkoxides [37,38]. During the first step, the hydrolysis of the precursor TEOS by water and NH_4OH as a catalyst formed reactive silanol groups and ethanol. In the next

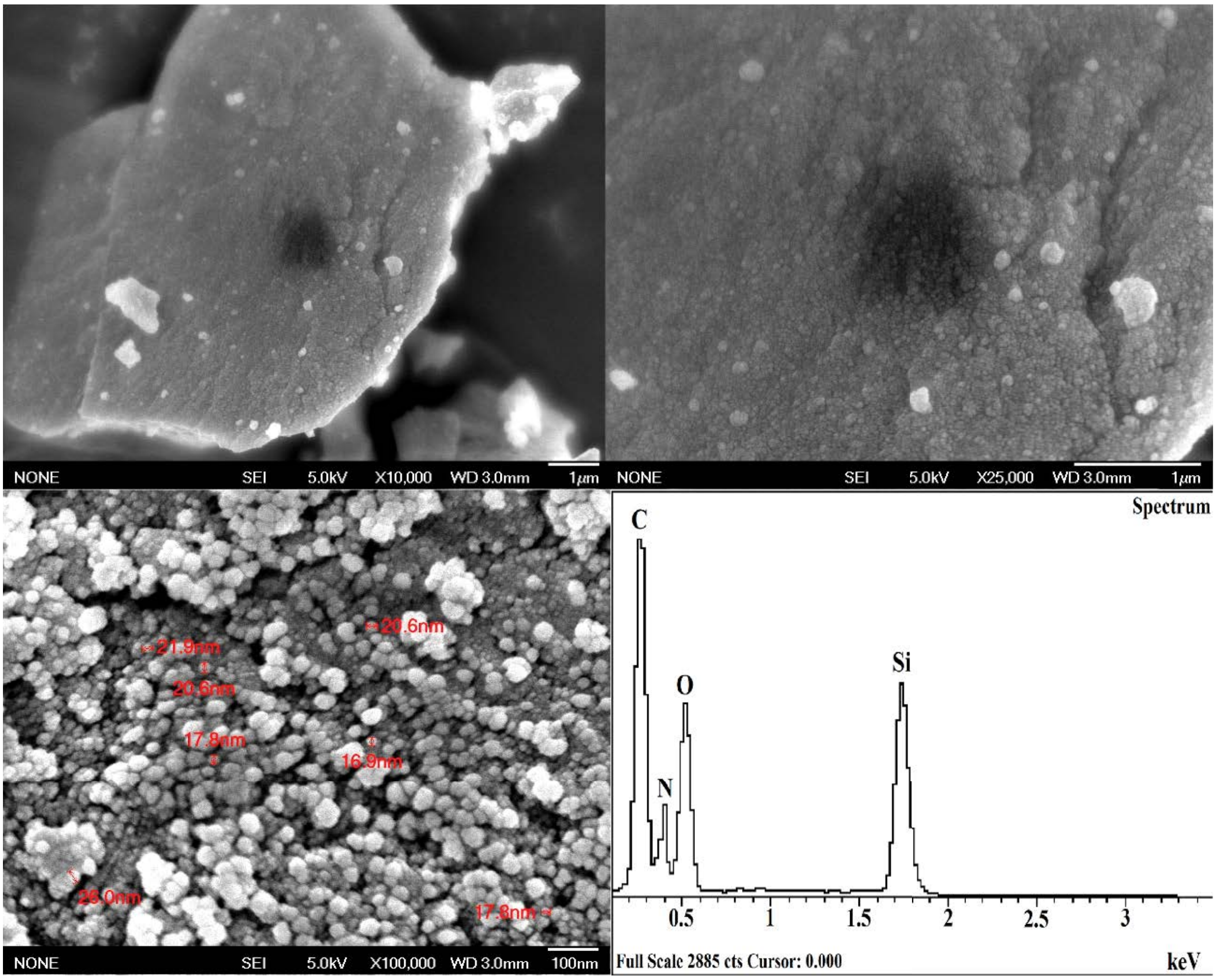

Fig. 2. FESEM micrograph of the CNPr@SiO_2 NP sorbent at ×50 K magnification and EDX spectra.

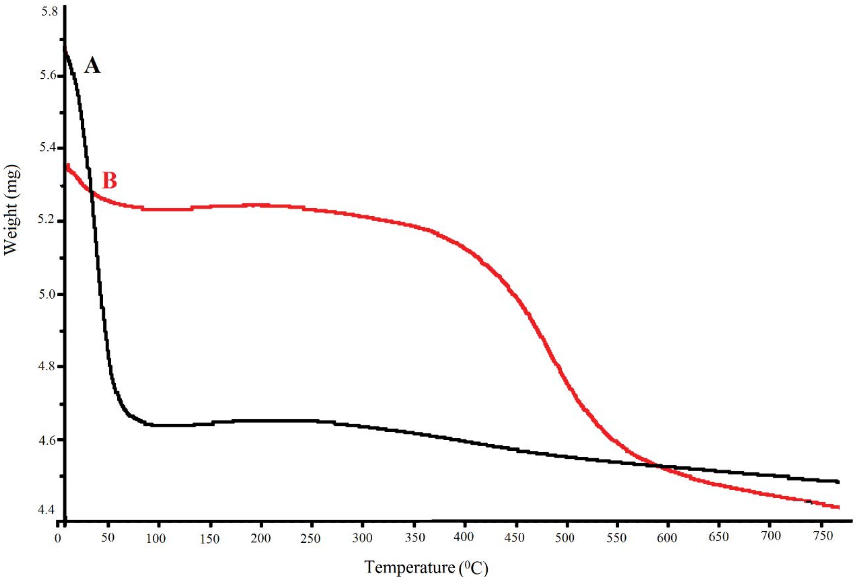

Fig. 3. TGA profiles of (A) SiO_2-NPs and (B) CNPr@SiO_2 NPs.

step, condensation/polycondensation process between the silanol groups or between silanol groups and ethoxy groups produced siloxane bridges (Si–O–Si) with the elimination of water and ethanol, respectively, which created silica nanoparticles. Finally, the prepared SiO_2 NPs were functionalized using CNPrTEOS by refluxing in toluene under nitrogen gas at 100°C for 24 h.

3.3. Adsorption mechanism of OPPs by CNPr@SiO_2 NPs

The experiment was conducted at pH 5.5 and based on pKa values the OPPs are stable at pH 5–7 for 24–15 d [39,40]. At acidic pH, OPPs undergo de-esterification and desetyl-OPPs/alcohol are the secondary products [41]. At alkaline pH, the OPPs are hydrolyzed to a secondary product of trichloro-2-pyridino (TCP) and diethylthiophosphoric acid (DETP) [41]. Fig. 4 shows that the CNPr@SiO_2 NP was able to extract polar dicrotophos better than the mid-polar diazinon and non-polar chlorpyrifos. This sorbent has a very high selectivity for the polar dicrotophos, which was mainly due to the special interactions between the analytes and the adsorbent as well as the high surface area and porous nature of the nanoparticles. The polar dicrotophos can be adsorbed by the CNPr@SiO_2 NPs through the hydrogen bonding formed between the OH groups present in the CNPr@SiO_2 NPs and the lone pair of electrons on the N atom, and the π–π interaction between the C≡N moiety and alkene double bond in dicrotophos. The nanosorbent was also able to extract the mid-polar diazinon and non-polar chlorpyrifos via the interaction with the propyl moiety with a higher response than the commercial CN SPE [42–44].

3.4. Optimization of the D-μ-SPE procedure

The extraction recovery in D-μ-SPE was dependent on the partitioning of analyte between the aqueous phase and the solid adsorbent. Therefore, six extraction parameters including mass of CNPr@SiO_2, desorption solvent type, desorption solvent volume, sample volumes, desorption time, and extraction time were investigated in order to optimize the OPPs extraction efficiencies. The experiments were carried out using a spiked water sample with OPPs at a concentration of 50 μg L^{-1} and in triplicates (the mean values were applied for data analysis).

3.4.1. Mass of the adsorbent

To investigate the effect of the amount of adsorbent on the extraction efficiency, the amount of CNPr@SiO_2 was varied from 25 to 125 mg. According to the results, the peak areas were increased when the amount of CNPr@SiO_2 was increased from 25 to 50 mg which can be due to the upsurge in active sites for adsorption (Fig. 5A) [45]. However, when 75 mg or higher amounts of the adsorbent was used, no further enhancement of the peak areas was observed. Thus, 50 mg of CNPr@SiO_2 was adopted for subsequent experiments.

3.4.2. Extraction time

Because the mass transfer is a time-dependent process, it is important to find the time needed for complete adsorption of the target analytes by the CNPr@SiO_2. The effect of the extraction time on the extraction efficiency was investigated by using various shaking times of 5, 10, 15, and 20 min. It was found that with increasing the extraction time to 10 min, the extraction efficiency reached a maximum and after that, the OPPs peak areas slightly decreased when the extraction time was prolonged to 20 min (Fig. 5B). This occurrence might be due to the back extraction of analytes from the adsorbent into the sample solution. Hence, an extraction time of 10 min was selected for the next experiments.

3.4.3. Desorption solvent type

In order to select an appropriate solvent for effective desorption of OPPs from the CNPr@SiO_2, some organic

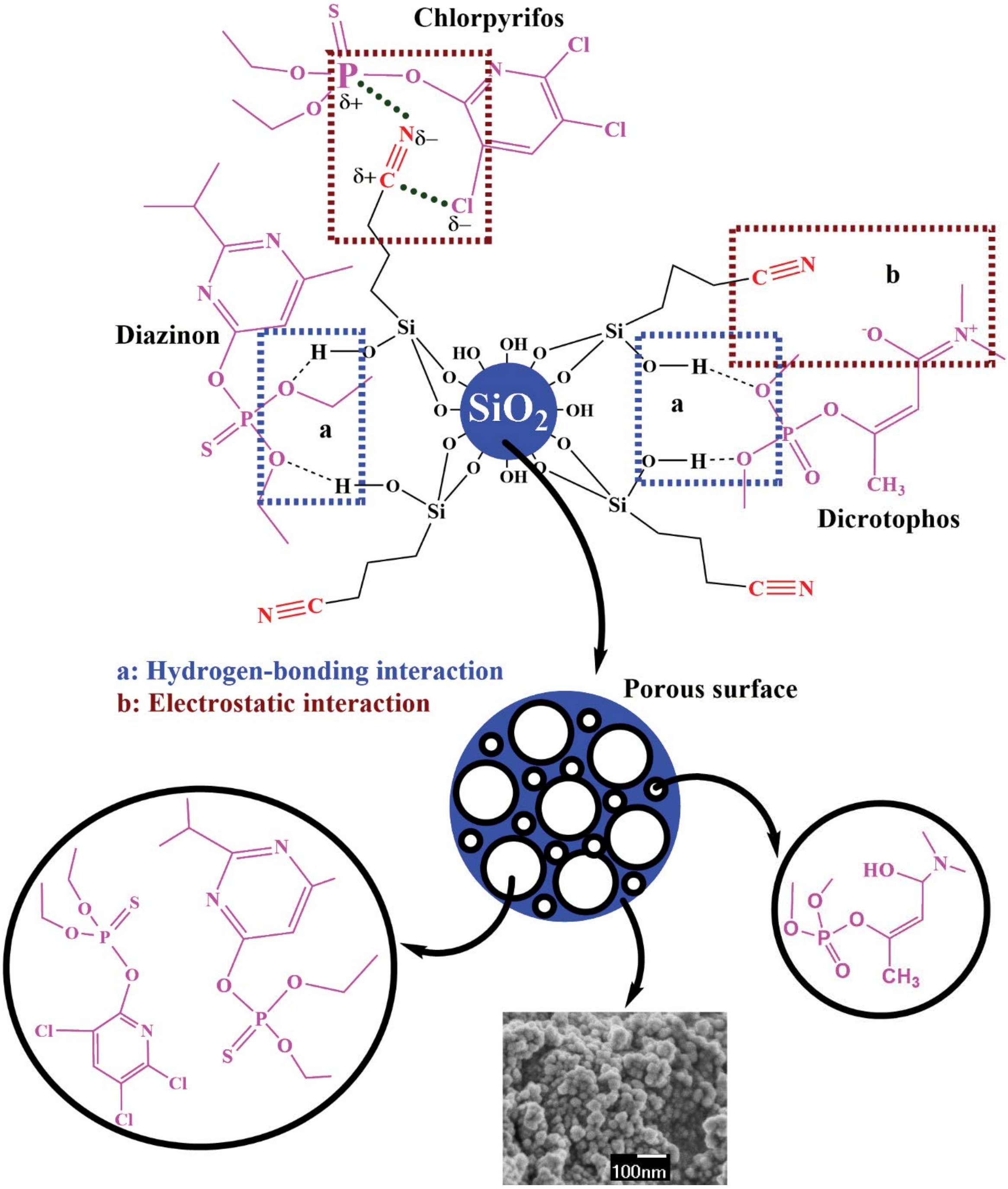

Fig. 4. Schematic of possible interactions of OPPs with CNPr@SiO_2 NPs adsorbent.

solvents including methanol, ethanol, dichloromethane, and *n*-hexane were used. The solvents have different polarities, with methanol being the most polar solvent and *n*-hexane being the most non-polar solvent. It was evident that dichloromethane provided the best extraction efficiency with the highest peak areas for the target OPPs (Fig. 5C). The other solvents were less effective for the desorption of the three selected OPPs. Thus, dichloromethane was used as the desorption solvent in subsequent experiments.

3.4.4. Volume of desorption solvent

Desorption solvent volume is an important extraction parameter as it should be enough to desorb effectively all OPPs from the D-µ-SPE sorbent. In this study, different volumes of the desorption solvent (DCM) were investigated from 100 to 300 µL to obtain the highest sensitivity with a minimum but sufficient eluent volume. Fig. 5D shows the optimization profile of desorption solvent volume. For the

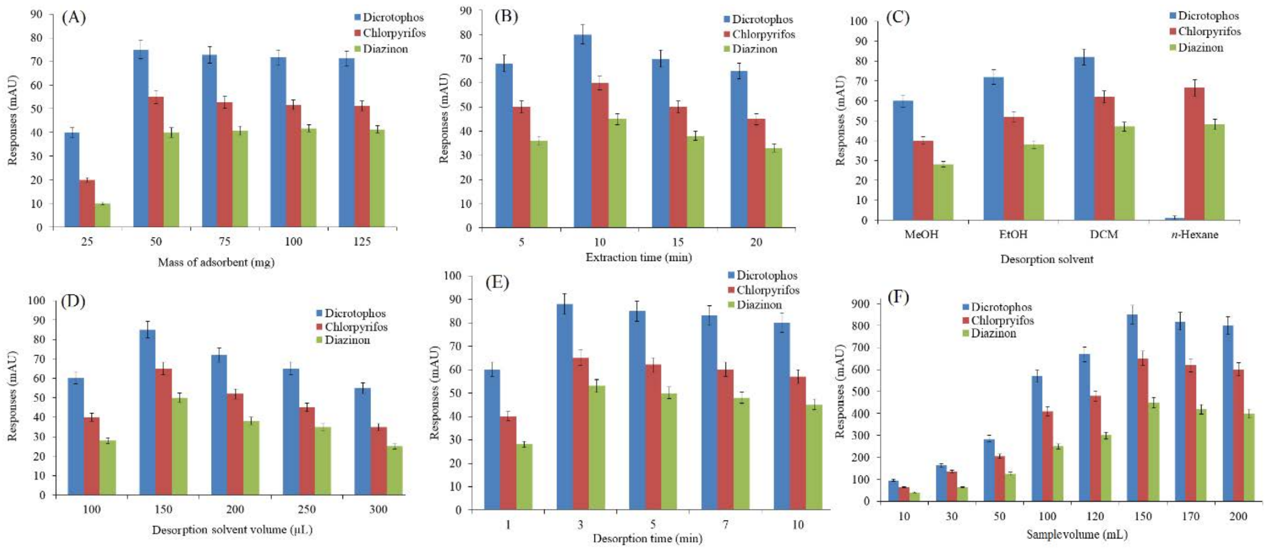

Fig. 5. Effect of (A) mass of adsorbent, (B) extraction time, (C) desorption solvent, (D) desorption solvent volume, (E) desorption time, and (F) different sample volumes on the CNPr@SiO$_2$ NPs-D-μ-SPE of OPPs from water samples.

proposed CNPr@SiO$_2$ NPs based D-μ-SPE method, 150 μL of dichloromethane was adequate for the satisfactory desorption of the trapped OPPs, as it gives the highest peak areas for all of the analytes, which means that the volume is sufficient to recover all of the OPPs studied.

3.4.5. Desorption time

The effect of desorption time was investigated by the ultrasonication of CNPr@SiO$_2$ NPs in dichloromethane for 1–10 min. It was observed that the maximum OPPs recoveries could be achieved in 3 min and no significant increase was observed after 3 min of ultrasonication (Fig. 5E). Therefore, a desorption time of 3 min was used in further experiments.

3.4.6. Sample volumes

The sample loading volume is the maximum volume of sample that can be loaded in a D-μ-SPE system and should be as large as possible to achieve the maximum sensitivity and enrichment of analytes. The sample volume was varied between 10 and 200 mL for the D-μ-SPE sorbent. Fig. 5F shows that the OPPs recoveries increased with increasing the sample from 10 to 150 mL. However, the peak areas of the OPPs were decreased when the sample volume was greater than 150 mL, probably due to the fact that the active sites in the CNPr@SiO$_2$ NPs were occupied by OPPs which decreased the adsorption of OPPs onto the surface of the adsorbent. Thus, the sample volume was set at 150 mL because it gave the highest peak areas for the target OPPs.

3.5. Reusability of the CNPr@SiO$_2$ NPs

The regeneration of the prepared CNPr@SiO$_2$ NPs was studied by performing repeated extraction runs until a significant decrease was observed in the analytes peak areas. After each run, the CNPr@SiO$_2$ NPs was washed consecutively with 5 mL of deionized water and 10 mL of methanol and reused for the next extraction. The experimental results indicated that the peak areas of CNPr@SiO$_2$ NPs were stable for up to at least 36 adsorption–desorption cycles. The high reusability was one of the major advantages of the prepared CNPr@SiO$_2$ NPs as a D-μ-SPE nano-adsorbent.

3.6. Method validation

The proposed D-μ-SPE method based on the laboratory made CNPr@SiO$_2$ NPs and the SPE technique by the commercial cyano-silica cartridge was evaluated by the linearity, limit of detection (LODs) (3 × SD/m) and limit of quantification (LOQs, 10 × SD/m). For this purpose, the spiking water samples at five different concentration levels of OPPs were prepared and analyzed according to the described procedure under the optimal experimental conditions. The calibration curves were constructed by plotting OPPs peak areas vs. concentrations. The results in Table 1 demonstrated good linearities achieved for CNPr@SiO$_2$ NPs based D-μ-SPE and commercial cyano-SiO$_2$ based SPE in the range of 0.16–100 and 5–50 μg L^{-1}, respectively, with coefficients of determination (R^2) higher than 0.9920. The LODs obtained for the CNPr@SiO$_2$ NPs based D-μ-SPE were 20–25 times lower than the LODs for CN-SPE which was probably due to the higher surface area and porous nature of the CNPr@SiO$_2$ nanoparticles compared to micro-sized CNPr-silica. The LODs values were found to be down to the ultra-trace level compared to the maximum residue limits (MRLs) set by the EU for OPPs in water samples. This proved that the developed D-μ-SPE SiO$_2$-NPs-CNPrTEOS method showed high sensitivity toward the selected OPPs. The method precision (RSDs %) was studied based on its repeatability (intra-batch) and reproducibility (inter-batch), which were in the ranges of 2.0%–3.1% and 1.5%–3.4%, respectively.

3.7. Determination of OPPs in water samples

The applicability of the developed D-μ-SPE method based on the CNPr@SiO$_2$ NPs was assessed by the analysis

Table 1
Qualitative data of the CNPr@SiO$_2$-NPs D-μ-SPE and CN-SPE analytical characteristics

OPPs	CNPr@SiO$_2$-NPs D-μ-SPE				CN-SPE			
	R^2	LOD (μg L^{-1})	LOQ (μg L^{-1})	LDR (μg L^{-1})	R^2	LOD (μg L^{-1})	LOQ (μg L^{-1})	LDR (μg L^{-1})
Dicrotophos	0.9925	0.047	0.158	0.16–100	0.9965	0.99	3.31	5–50
Diazinon	0.9935	0.059	0.199	0.20–100	0.9944	1.52	5.06	5–50
Chlorpyrifos	0.9982	0.056	0.187	0.20–100	0.9920	1.26	4.20	5–50

of various water samples. No residue of the OPPs was detected in all water samples analyzed. To test the accuracy, all water samples were spiked at 0.2 μg L^{-1} of OPPs, and recoveries were calculated. Table 2 shows the percentage recoveries (with corresponding RSDs) obtained by two methods for water samples. The CNPr@SiO$_2$ NPs based D-μ-SPE showed good recoveries between 101.21% and 109.12% with RSDs ranged from 0.20% to 6.70%. The results indicated that the developed D-μ-SPE using the CNPr@SiO$_2$ NPs is accurate enough for the extraction of the three selected OPPs in water samples. Figs. 6a and b present the chromatograms of the analyzed blank and spiked tap water, respectively.

3.8. Comparison of D-μ-SPE with other methods

The analytical performances of the CNPr@SiO$_2$ NPs based D-μ-SPE were compared with some previously reported sample preparation methods for the extraction of OPPs [46,47]. The results were summarized in Table 3. The developed D-μ-SPE exhibited low LODs and good recoveries for the separation of OPPs from aqueous media. Although DSPE based on MWCNTs showed lower LODs for OPPs, this result is possibly related to the strong π–π interactions between the benzene rings of OPPs (i.e., chlorpyrifos) and the π–π system of MWCNTs and use of a highly sensitive and selective detector (MS/MS) [42]. Other methods also showed good recoveries and satisfactory LODs for the extraction of OPPs from complex matrices, but some of these methods are tedious and consume large volumes of organic solvents. The proposed D-μ-SPE method showed high recoveries, consumed less solvent, had a high enrichment factor (2,500×), and lower LODs in comparison to MRLs set by the EU. The method utilized a minimum amount of mesoporous silica compared to other SPE methods. In addition, the high surface area of the CNPr@SiO$_2$ nanoparticles (570 m^2 g^{-1}) provided enormous active sites available for the adsorption of OPPs, leading to the high recoveries which were comparable to those for a commercially available SPE sorbent. Furthermore, a low amount of organic solvent (150 μL) required in the developed D-μ-SPE makes it superior to SPE.

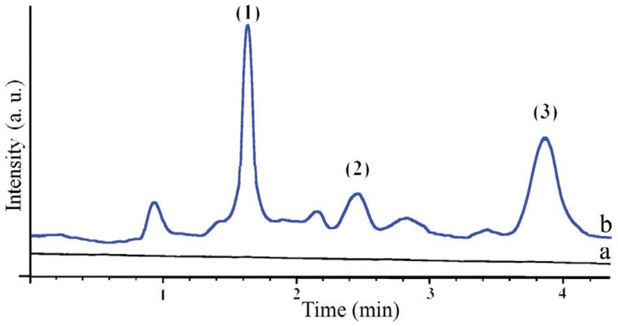

Fig. 6. Chromatograms obtained using CNPr@SiO$_2$ NPs based D-μ-SPE-HPLC-UV analysis of the OPPs in tap water samples (a) unspiked and (b) tap water sample spiked at 0.2 μg L^{-1}. Peaks: (1) dicrotophos, (2) diazinon, and (3) chlorpyrifos.

Table 2
Analysis of water samples using the developed CNPr@SiO$_2$-NPs D-μ-SPE and commercial CN-SPE methods with HPLC-UV

Sample	OPP	CNPr@SiO$_2$-NPs-D-μ-SPE recovery% (RSD%)	CN SPE recovery% (RSD%)
Tap water	Dicrotophos	102.86 (5.96)	98.36 (5.50)
	Diazinon	106.66 (6.33)	101.57 (5.22)
	Chlorpyrifos	105.46 (5.77)	96.45 (2.99)
Drinking water	Dicrotophos	109.12 (4.12)	94.76 (5.47)
	Diazinon	109.27 (6.70)	103.94 (4.38)
	Chlorpyrifos	107.45 (4.31)	96.45 (4.16)
Mineral water	Dicrotophos	106.98 (0.21)	95.11 (5.33)
	Diazinon	105.57 (0.22)	100.98 (2.29)
	Chlorpyrifos	101.92 (0.20)	96.94 (6.70)
River water	Dicrotophos	103.43 (3.89)	90.69 (5.98)
	Diazinon	101.21 (2.82)	97.42 (4.52)
	Chlorpyrifos	104.00 (5.20)	89.83 (5.98)

Table 3
Comparison of LODs and percentage recoveries of the proposed CNPr@SiO_2-NPs-D-μ-SPE with other methods for OPPs extraction

Method	Detection	Adsorbent	Sample	Analyte	LOD	%Recovery	References
DSPE	GC-MS/MS	MWVNTs	Tea	78 pesticide	0.01 μg L^{-1}	66.8–112	[46]
DSPE	GC-MS	MWCNTs/alumina	Oil	Diazinon, Malathion, Fenthion	0.7 μg kg^{-1}	85–114	[47]
SPE	GC-FPD	Mesoporous alumina	Vegetables, fruits, and tea	Dichlorvos, Chlorpyrifos, Fenthion, Methamidophos	0.79 μg kg^{-1}	83–103	[48]
DSPE	HPLC-MS/MS	Graphitized carbon	Milk	44 pesticides	0.4 μg L^{-1}	>75%	[49]
DSPE	GC–FPD	PSA and GCB	Soil	Diazinon, Disulfoton, Chlorpyrifos, Fenthion	0.2 ng g^{-1}	79–106	[50]
DSPE	GC-FPD	PSA and C18	Cereal grains	Dichlorvos, Diazinon, Disulfoton, Chlorpyrifos, Fenthion	1.00 μg kg^{-1}	57.7–98.1	[51]
SPE	HPLC-UV	Imprinted polymers	Water	Diazinon	3.00 μg L^{-1}	77–98	[52]
SPE	HPLC-UV	Imprinted polymers	Vegetables	Trichlorfon and Monocrotophos	1.2 μg L^{-1}	88.5–94.2	[53]
SPE	HPLC-UV	CNPrTEOS	Water	Dicrotophos, Diazinon, Chlorpyrifos	0.072 μg L^{-1}	80.1–92.1	[54]
MSPE	HPLC-UV	Fe_3O_4 MNPs	Beverage	Metalaxyl, Dimethomorph, Kresoxim-methyl, Flusilazole	5.0 μg L^{-1}	70.6–106.8	[55]
D-μ-SPE	HPLC-UV	SiO_2-NPs-CNPrTEOS	Water	Dicrotophos, Diazinon, Chlorpyrifos	0.047 μg L^{-1}	101–109	This study

Moreover, CNPr@SiO_2 NPs – D-μ-SPE has the advantage of a simplified analytical sample preparation process without using any expensive or sophisticated apparatus.

4. Conclusion

In this study, cyanopropyl functionalized nanosilica (CNPr@SiO_2 NPs) has been successfully prepared and applied as a promising adsorbent for D-μ-SPE of three OPPs with different polarities from water samples. Besides the high selectivity of the CNPr@SiO_2 NPs for the polar pesticide, it could also extract non-polar OPPs with satisfactory recoveries, which was most likely owing to the high surface area and mesoporous nature of the nanoparticles. The D-μ-SPE method using the CNPr@SiO_2 nanosorbent offers better analytical performances than commercial CN-SPE cartridge with good accuracy (recoveries: 101.21%–109.12%) and precision (RSD < 7%) for the selected real water samples. The dispersed adsorbent into the aqueous solution in the D-μ-SPE method enables the analytes to contact easily with the nanosorbent particles, achieving a greater capacity per mass of sorbent consumed and avoiding the channeling or blocking of the cartridge that happens in SPE. The developed method allowed the extraction of OPPs with a low amount of solvent (150 μL) and mass of nanosorbent (50 mg) within 10 min of extraction time. Therefore, this method permits the monitoring of OPPs residues in water samples well below permissible levels set by regulations.

Acknowledgments

The authors would like to thank Ministry of Education (MOE) Malaysia and University Teknologi Malaysia for financial support through the Research Grants R.J130000. 7826.3F452, Q.J130000.2526.04H22 and Q.J130000. 526.01H94. Z. Sotoudehnia also thanks UTM for the International Doctorate Fellowship (IDF) received.

References

[1] L. Liang, X. Wang, Y. Sun, P. Ma, X. Li, H. Piao, Y. Jiang, D. Song, Magnetic solid-phase extraction of triazine herbicides from rice using metal-organic framework MIL-101(Cr) functionalized magnetic particles, Talanta, 179 (2018) 512–519.
[2] M. Naushad, G. Sharma, Z.A. Alothman, Photodegradation of toxic dye using Gum Arabic-crosslinked-poly(acrylamide)/ $Ni(OH)_2$/FeOOH nanocomposites hydrogel, J. Cleaner Prod., 241 (2019) 118263.
[3] W. Wang, X. Ma, Q. Wu, C. Wang, X. Zang, Z. Wang, The use of graphene-based magnetic nanoparticles as adsorbent for the extraction of triazole fungicides from environmental water, J. Sep. Sci., 35 (2012) 2266–2272.
[4] W. Wang, Y. Li, Q. Wu, C. Wang, X. Zang, Z. Wang, Extraction of neonicotinoid insecticides from environmental water samples with magnetic graphene nanoparticles as adsorbent followed by determination with HPLC, Anal. Methods, 4 (2012) 766–772.
[5] A. Kumar, G. Sharma, M. Naushad, T. Ahamad, R.C. Veses, F.J. Stadler, Highly visible active Ag_2CrO_4/Ag/$BiFeO_3$@RGO nano-junction for photoreduction of CO_2 and photocatalytic removal of ciprofloxacin and bromate ions: the triggering effect of Ag and RGO, J. Chem. Eng., 370 (2019) 148–165.
[6] J. Xie, T. Liu, G. Song, Y. Hu, C. Deng, Simultaneous analysis of organophosphorus pesticides in water by magnetic solid-phase extraction coupled with GC–MS, Chromatographia, 76 (2013) 535–540.

[7] S. Mahpishanian, H. Sereshti, M. Baghdadi, Superparamagnetic core-shells anchored onto graphene oxide grafted with phenylethyl amine as a nano-adsorbent for extraction and enrichment of organophosphorus pesticides from fruit, vegetable and water samples, J. Chromatogr. A, 1406 (2015) 48–58.

[8] G. Sharma, A. Kumar, K. Devi, S. Sharma, M. Naushad, A.A. Ghfar, T. Ahamad, F.J. Stadler, Guar gum-crosslinked-Soya lecithin nanohydrogel sheets as effective adsorbent for the removal of thiophanate methyl fungicide, Int. J. Biol. Macromol., 114 (2018) 295–305.

[9] G. Yang, Z. He, X. Liu, C. Liu, J. Zhan, D. Liu, P. Wang, Z. Zhou, Polymer-coated magnetic nanospheres for preconcentration of organochlorine and pyrethroid pesticides prior to their determination by gas chromatography with electron capture detection, Microchim. Acta, 183 (2016) 1187–1194.

[10] M.A. Farajzadeh, M.R. Afshar Mogaddam, S. Rezaee Aghdam, N. Nouri, M. Bamorrowat, Application of elevated temperature-dispersive liquid-liquid microextraction for determination of organophosphorus pesticides residues in aqueous samples followed by gas chromatography-flame ionization detection, Food Chem., 212 (2016) 198–204.

[11] S. Moinfar, M.R.M. Hosseini, Development of dispersive liquid-liquid microextraction method for the analysis of organophosphorus pesticides in tea, J. Hazard. Mater., 169 (2009) 907–911.

[12] L.M. Ravelo-Pérez, J. Hernández-Borges, M.A. Rodríguez-Delgado, Multi-walled carbon nanotubes as efficient solid-phase extraction materials of organophosphorus pesticides from apple, grape, orange and pineapple fruit juices, J. Chromatogr. A, 1211 (2008) 33–42.

[13] L. Zhang, Y. Wang, C. Sun, S. Yang, H. He, Simultaneous determination of organochlorine, organophosphorus, and pyrethroid pesticides in bee pollens by solid-phase extraction cleanup followed by gas chromatography using electron-capture detector, Food Anal. Methods, 6 (2012) 1508–1514.

[14] Q. Han, Z. Wang, J. Xia, X. Zhang, H. Wang, M. Ding, Application of graphene for the SPE clean-up of organophosphorus pesticides residues from apple juices, J. Sep. Sci., 37 (2014) 99–105.

[15] D.A. Lambropoulou, T.A. Albanis, Headspace solid phase microextraction applied to the analysis of organophosphorus insecticides in strawberry and cherry juices, J. Agric. Food Chem., 50 (2002) 3359–3365.

[16] M. Farajzadeh, M. Hatami, Solid-phase microextraction gas chromatography for determination of some organophosphorus pesticides, Chromatographia, 59 (2004) 259–262.

[17] J. Chen, C. Duan, Y. Guan, Sorptive extraction techniques in sample preparation for organophosphorus pesticides in complex matrices., J. Chromatogr. B, 878 (2010) 1216–1225.

[18] H. Heidari, H. Razmi, Multi-response optimization of magnetic solid phase extraction based on carbon coated Fe_3O_4 nanoparticles using desirability function approach for the determination of the organophosphorus pesticides in aquatic samples by HPLC-UV, Talanta 99 (2012) 13–21.

[19] Z. Xiong, L. Zhang, R. Zhang, Y. Zhang, J. Chen, W. Zhang, Solid-phase extraction based on magnetic core-shell silica nanoparticles coupled with gas chromatography-mass spectrometry for the determination of low concentration pesticides in aqueous samples, J. Sep. Sci., 35 (2012) 2430–2437.

[20] Y. Li, L. Qi, Y. Shen, H. Ma, Facile preparation of surface-exchangeable core@shell iron oxide@gold nanoparticles for magnetic solid-phase extraction: use of gold shell as the intermediate platform for versatile adsorbents with varying self-assembled monolayers, Anal. Chim. Acta, 811 (2014) 36–42.

[21] S. Mahpishanian, H. Sereshti, Graphene oxide-based dispersive micro-solid phase extraction for separation and preconcentration of nicotine from biological and environmental water samples followed by gas chromatography-flame ionization detection, Talanta, 130 (2014) 71–77.

[22] F. Galán-Cano, R. Lucena, S. Cárdenas, M. Valcárcel, Dispersive micro-solid phase extraction with ionic liquid-modified silica for the determination of organophosphate pesticides in water by ultra performance liquid chromatography, Microchem. J., 106 (2013) 311–317.

[23] B. Peng, J. Zhang, R. Lu, S. Zhang, W. Zhou, H. Gao, Dispersive micro-solid phase extraction based on self-assembling, ionic liquid-coated magnetic particles for the determination of clofentezine and chlorfenapyr in environmental water samples, Analyst, 138 (2013) 6834–6843.

[24] K. Pyrzynska, Use of nanomaterials in sample preparation, Trends Anal. Chem., 43 (2013) 100–108.

[25] R. Lucena, B.M. Simonet, S. Cárdenas, M. Valcárcel, Potential of nanoparticles in sample preparation, J. Chromatogr. A, 1218 (2011) 620–637.

[26] J. Tian, J. Xu, F. Zhu, T. Lu, C. Su, G. Ouyang, Application of nanomaterials in sample preparation, J. Chromatogr. A, 1300 (2013) 2–16.

[27] M.M. Kalhor, A.A. Rafati, L. Rafati, A.A. Rafati, Synthesis, characterization and adsorption studies of amino functionalized silica nano hollow sphere as an efficient adsorbent for removal of imidacloprid pesticide, J. Mol. Liq., 266 (2018) 453–459.

[28] H. Bagheri, A. Roostaie, E. Babanezhad, New grafted nanosilica-based sorbent for needle trap extraction of polycyclic aromatic hydrocarbons from water samples followed by GC/MS, Chromatographia, 74 (2011) 429–436.

[29] F. Wei, X. Liu, M. Zhai, Z. Cai, G. Xu, J. Yang, S. Du, Q. Hu, Molecularly imprinted nanosilica solid-phase extraction for bisphenol a in fish samples, Food Anal. Methods, 6 (2013) 415–420.

[30] M.E. Mahmoud, M.F. Amira, A.A. Zaghloul, G.A.A. Ibrahim, High performance microwave-enforced solid phase extraction of heavy metals from aqueous solutions using magnetic iron oxide nanoparticles-protected-nanosilica, Sep. Purif. Technol., 163 (2016) 169–172.

[31] M. Llaver, E.A. Coronado, R.G. Wuilloud, High performance preconcentration of inorganic Se species by dispersive micro-solid phase extraction with a nanosilica-ionic liquid hybrid material, Spectrochim. Acta, Part B, 138 (2017) 23–30.

[32] M.I. Youssif, R.M. El-Maghraby, S.M. Saleh, A.A. Elgibaly, Sol–gel tailored synthesized nanosilica for enhanced oil recovery in water-wet and oil-wet benthemier sandstone, Energy Fuels, 32 (2018) 12373–12382.

[33] Z. Lu, W. Hu, F. Xie, L. Zhuo, B. Yang, Sol-gel synthesis of nanosilica-coated: para-aramid fibers and their application in the preparation of paper-based friction materials, RSC Adv., 7 (2017) 30632–30639.

[34] G. Sharma, V.K. Gupta, S. Agarwal, S. Bhogal, M. Naushad, A. Kumar, F.J. Stadler, Fabrication and characterization of trimetallic nano-photocatalyst for remediation of ampicillin antibiotic, J. Mol. Liq., 260 (2018) 342–350.

[35] D. Yang, Y. Xu, D. Wu, Y. Sun, H. Zhu, F. Deng, Super hydrophobic mesoporous silica with anchored methyl groups on the surface by a one-step synthesis without surfactant template, J. Phys. Chem. C, 111 (2007) 999–1004.

[36] M. Naushad, G. Sharma, A. Kumar, S. Sharma, A.A. Ghfar, A. Bhatnagar, F.J. Stadler, M.R. Khan, Efficient removal of toxic phosphate anions from aqueous environment using pectin based quaternary amino anion exchanger, Int. J. Biol. Macromol., 106 (2018) 1–10.

[37] M.A. Aegerter, M. Mennig, Sol-Gel technologies for Glass Producers and Users, Springer Science & Business Media, New York, 2013.

[38] A. Kumar, A. Kumar, G. Sharma, A.H. Al-Muhtaseb, M. Naushad, A.A. Ghfar, F.J. Stadler, Quaternary magnetic $BiOCl/g-C_3N_4/Cu_2O/Fe_3O_4$ nano-junction for visible light and solar powered degradation of sulfamethoxazole from aqueous environment, J. Chem. Eng., 334 (2018) 462–478.

[39] J. Farmer, E. Webb, R. Pierce, K. Bradley, Evaluating the potential for weed seed dispersal based on waterfowl consumption and seed viability, Pest Manage. Sci., 73 (2017) 2592–2603.

[40] B. Liu, L.L. McConnell, A. Torrents, Hydrolysis of chlorpyrifos in natural waters of the chesapeake bay, Chemosphere, 44 (2001) 1315–1323.

[41] M. Svobodová, K. Šmídová, M. Hvězdová, J. Hofman, Uptake kinetics of pesticides chlorpyrifos and tebuconazole in the

earthworm eisenia andrei in two different soils, Environ Pollut., 236 (2018) 257–264.

[42] S. Kulkarni, L. Fang, K. Alhooshani, A. Malik, Sol-Gel immobilized cyano-polydimethylsiloxane coating for capillary microextraction of aqueous trace analytes ranging from polycyclic aromatic hydrocarbons to free fatty acids, J. Chromatogr. A, 1124 (2006) 205–216.

[43] G. Sharma, M. Naushad, A.H. Al-Muhtaseb, A. Kumar, M.R. Khan, S. Kalia, Shweta, M. Bala, A. Sharma, Fabrication and characterization of chitosan-crosslinked-poly(alginic acid) nanohydrogel for adsorptive removal of Cr(VI) metal ion from aqueous medium, Int. J. Biol. Macromol., 95 (2017) 484–493.

[44] G. Sharma, M. Naushad, A. Kumar, S. Rana, S. Sharma, A. Bhatnagar, F.J. Stadler, A.A. Ghfar, M.R. Khan, Efficient removal of coomassie brilliant blue R-250 dye using starch/poly(alginic acid-cl-acrylamide) nanohydrogel, J. Process. Saf. Environ., 109 (2017) 301–310.

[45] G. Sharma, M. Naushad, Adsorptive removal of noxious cadmium ions from aqueous medium using activated carbon/zirconium oxide composite: Isotherm and kinetic modelling, J. Mol. Liq., 310 (2020) 11325, doi: 10.1016/j.molliq.2020.113025.

[46] X. Hou, S. Lei, S. Qiu, L. Guo, S. Yi, W. Liu, A multi-residue method for the determination of pesticides in tea using multi-walled carbon nanotubes as a dispersive solid phase extraction absorbent, Food Chem., 153 (2014) 121–129.

[47] R. Su, X. Xu, X. Wang, D. Li, X. Li, H. Zhang, A. Yu, Determination of organophosphorus pesticides in peanut oil by dispersive solid phase extraction gas chromatography–mass spectrometry, J. Chromatogr. B, 879 (2011) 3423–3428.

[48] Y. Hu, C. Xi, S. Cao, G. Wang, X. Li, L. Zhang, Y. Zhang, Simultaneous determination of 16 organophosphorous pesticides in vegetables, fruits and tea by gas chromatography coupled with clean-up by mesoporous alumina as solid-phase extraction adsorbent, Chin. J. Chromatogr., 32 (2014) 784–788.

[49] T. Dagnac, M. Garcia-Chao, P. Pulleiro, C. Garcia-Jares, M. Llompart, Dispersive solid-phase extraction followed by liquid chromatography–tandem mass spectrometry for the multi-residue analysis of pesticides in raw bovine milk, J. Chromatogr. A, 1216 (2009) 3702–3709.

[50] Q. Wang, J. Yin, H. Pan, F. Xu, Y. Yang, A novel method based on combining ultrasonic-assisted dispersive solid-phase extraction and low-density solvent dispersive liquid–liquid microextraction (UA-DSPE-LDS-DLLME) for the determination of organophosphorus pesticides in soil, Anal. Methods, 6 (2014) 7335–7342.

[51] C. Jia, X. Zhu, J. Wang, E. Zhao, M. He, L. Chen, P. Yu, Combination of dispersive solid-phase extraction and salting-out homogeneous liquid–liquid extraction for the determination of organophosphorus pesticides in cereal grains, J. Sep. Sci., 37 (2014) 1862–1866.

[52] D. Davoodi, M. Hassanzadeh-Khayyat, M.A. Rezaei, S.A. Mohajeri, Preparation, evaluation and application of diazinon imprinted polymers as the sorbent in molecularly imprinted solid-phase extraction and liquid chromatography analysis in cucumber and aqueous samples, Food Chem., 158 (2014) 421–428.

[53] X. Wang, Q. Tang, Q. Wang, X. Qiao, Z. Xu, Study of a molecularly imprinted solid-phase extraction coupled with high-performance liquid chromatography for simultaneous determination of trace trichlorfon and monocrotophos residues in vegetables, J. Sci. Food Agric., 94 (2014) 1409–1415.

[54] Z. Soutoudehnia Korrani, W.A. Wan Ibrahim, H. Rashidi Nodeh, H.Y. Aboul-Enein, M.M. Sanagi, Simultaneous pre-concentration of polar and non-polar organophosphorus pesticides from water samples by using a new sorbent based on mesoporous silica, J. Sep. Sci., 39 (2016) 1144–1151.

[55] M. Tian, D.X. Chen, Y.L. Sun, Y.-W. Yang, Q. Jia, Pillararene-functionalized Fe_3O_4 nanoparticles as magnetic solid-phase extraction adsorbent for pesticide residue analysis in beverage samples, RSC Adv., 3 (2013) 22111–22119.